Journal of Magnetism and Magnetic Materials 394 (2015) 37–43

Contents lists available at ScienceDirect

Journal of Magnetism and Magnetic Materials

journal homepage: www.elsevier.com/locate/jmmm

Coexistence of short- and long-range ferromagnetic order in nanocrystalline $Fe_2Mn_{1-x}Cu_xAl$ ($x=0.0$, 0.1 and 0.3) synthesized by high-energy ball milling

Tran Dang Thanh [a,*], Dwi Nanto [b], Ngo Thi Uyen Tuyen [c], Wen-Zhe Nan [d], YiKyung Yu [e], Daniel M. Tartakovsky [e,*], S.C. Yu [d,*]

[a] Institute of Materials Science, Vietnam Academy of Science and Technology, 18 Hoang Quoc Viet, Hanoi, Vietnam
[b] Physics Education, Syarif Hidayatullah States Islamic University, Jakarta 15412, Indonesia
[c] Department of Natural Science, Nha Trang Pedagogic College, Nguyen Chanh, Nha Trang, Khanh Hoa, Vietnam
[d] Department of Physics, Chungbuk National University, Cheongju 361-763, Korea
[e] Department of Mechanical and Aerospace Engineering, University of California, San Diego, CA 92093-0411, USA

ARTICLE INFO

Article history:
Received 31 January 2015
Received in revised form
15 June 2015
Accepted 17 June 2015
Available online 19 June 2015

Keywords:
Nanocrystalline
Critical behavior
Heusler alloy

ABSTRACT

In this work, we prepared nanocrystalline $Fe_2Mn_{1-x}Cu_xAl$ ($x=0.0$, 0.1 and 0.3) powders by the high energy ball milling technique, and then studied their critical properties. Our analysis reveals that the increase of Cu-doping concentration (up to $x=0.3$) in these powders leads to a gradual increase of the ferromagnetic–paramagnetic transition temperature from 406 to 452 K. The Banerjee criterion suggests that all the samples considered undergo a second-order phase transition. A modified Arrott plot and scaling analysis indicate that the critical exponents ($\beta=0.419$ and 0.442, $\gamma=1.082$ and 1.116 for $x=0.0$ and 0.1, respectively) are located in between those expected for the 3D-Heisenberg and the mean-field models; the values of $\beta=0.495$ and $\gamma=1.046$ for $x=0.3$ sample are very close to those of the mean-field model. These features reveal the coexistence of the short- and long-range ferromagnetic order in the nanocrystalline $Fe_2Mn_{1-x}Cu_xAl$ powders. Particularly, as the concentration of Cu increases, values of the critical exponent shift towards those of the mean-field model. Such results prove the Cu doping favors establishing a long-range ferromagnetic order.

1. Introduction

Heusler alloys are thought to have a wide range of thermoelectric [1,2], spintronics [3,4], and magnetocaloric [5–7] applications. This is because Co_2MnSi Heusler alloys are experimentally shown to be half-metallic; and the phenomenon of half-metallic magnetism plays a crucial role in magnetoelectronics and spintronics [8], both of which are at the forefront of modern nanoscience [9]. These alloys possess a giant tunneling magnetoresistance ratio of 570% that has been observed at 2 K in Co_2MnSi/Al–O/Co_2MnSi magnetic tunnel junction [10]. A half-metallic magnetic material exhibits a usual metallic behavior for the one spin direction, while an energy gap in the band structure is present in other spin directions similarly to semiconductors [11,12]. The borderline between magnetoelectronics and spintronics is flexible [13].

Most studies of the magnetocaloric effect (MCE) in Heusler alloys deal with low temperatures not exceeding room temperature. Unfortunately, there are a few work reported for above room temperature. Among the few high-temperature studies, the MCE was observed in an $Ni_{49}Mn_{39}Sb_{12}$ alloy at around 347 K (with the maximum magnetic entropy change $|\Delta S_{max}|=5.2$ J kg^{-1} K^{-1} under an applied magnetic field change $H=50$ kOe) [14] and in an $Ni_{0.5}Mn_{0.3}Sb_{0.2}$ alloy at around 342 K (with $|\Delta S_{max}|=1.0$ J kg^{-1} K^{-1} under $H=12$ kOe) [15]. Even less attention has been paid to Fe-based Heusler alloys. A notable exception is the study of FeMnGa alloys [16], which found a strong hysteresis due to the fact that the martensitic phase induced by the applied field cannot be completely recovered to austenite when the magnetic field decreases to zero.

In this paper, we present a detailed analysis of critical properties near the ferromagnetic (FM)–paramagnetic (PM) phase transition of nanocrystalline $Fe_2Mn_{1-x}Cu_xAl$ ($x=0.0$, 0.1 and 0.3) powders by using the modified Arrott plots (MAP) [17], the

* Corresponding authors.
E-mail addresses: thanhxraylab@yahoo.com (T.D. Thanh), dmt@ucsd.edu (D.M. Tartakovsky), scyu@cbnu.ac.kr (S.C. Yu).

http://dx.doi.org/10.1016/j.jmmm.2015.06.036
0304-8853/

Kouvel–Fisher (KF) [18], and the universal mater curve [19] methods. A comparison of the critical exponents β, γ and T_C obtained from the MAP and KF methods reveals that these values agree very well. Our analysis points to the coexistence of short- and long-range FM interactions in nanocrystalline $Fe_2Mn_{1-x}Cu_xAl$. Further, Cu doping in nanocrystalline $Fe_2Mn_{1-x}Cu_xAl$ favors establishment of a long-range FM order.

2. Experiments

Nanocrsytalline $Fe_2Mn_{1-x}Cu_xAl$ (x=0.0, 0.1 and 0.3) powders synthesized by means of high-energy ball milling technique, high-purity powder metals of Fe, Cu, Mn and Al (99.9%) were used as precursors. Stoichiometric ratios of the starting materials were mixed and milled for 96 h by a mechanical ball milling (SPEX 8000D with speed of 875 rpm). In this step, we used stainless-steel balls and vial. The starting materials were put in a vial (volume 65 cm^3), here the weighted ratio between balls and sample was about 8:1. The milling processes were carried out in an Argon atmosphere. After that, the room temperature crystal structure of the final products was checked by an X-ray diffractometer (Brucker AXS, D8 Discover) using a Cu-K_α radiation source. The magnetic measurements versus temperature and external magnetic field were performed on a vibrating sample magnetometer (VSM-Lakeshore 331).

3. Results and discussion

The X-ray diffraction (XRD) patterns of samples are shown in Fig. 1. It appears that the nanocsrytalline $Fe_2Mn_{1-x}Cu_xAl$ powders successfully prepared had a single phase. The Miller-indexed XRD peaks correspond to W-type structure disorder in full Heusle alloy belonging to the space group Im-3m [20]. By using the Scherrer–Debye formula, $d=K\lambda/\beta_S\cos\theta$, the average value of the nanocrystalline size (d) can be obtained, where β_S is the full-width at half-maximum (FWHM) of an XRD peak, θ is Bragg angle, and K=0.9 is the shape factor. In this wok, we used (1 1 1) XRD peak to estimate the values of d for samples. Thus, the values of d are found to be about 10 nm for all the samples.

In Fig. 2, it shows the temperature dependences of normalized magnetization $M(T)/M_{max}$ for nanocsrytalline $Fe_2Mn_{1-x}Cu_xAl$ powders in an applied magnetic field of 100 Oe. One can see that with increasing temperature, all the samples reveal a steep FM–PM phase transition. Experimentally, it was found that this phase transition can be shifted to higher temperatures by increasing the Cu concentration. Here, the T_C values determined from the minimum of the dM/dT versus T curves are 406, 413 and 449 K for

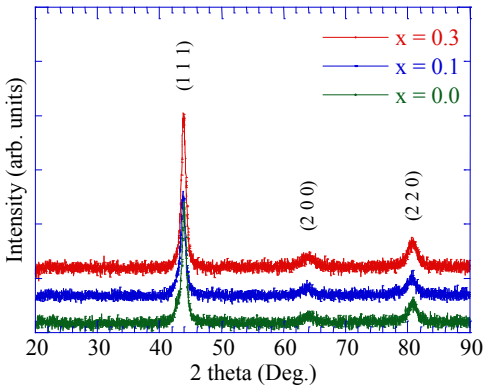

Fig. 1. XRD patterns for nanocrystalline $Fe_2Mn_{1-x}Cu_xAl$ powders.

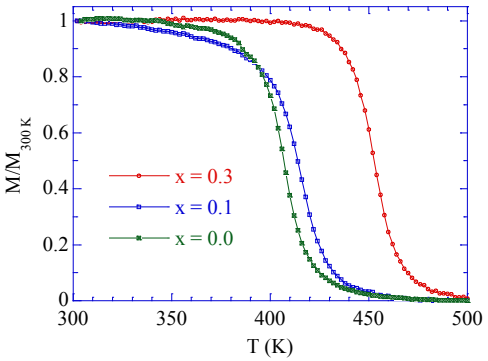

Fig. 2. $M(T)/M_{300\ K}$ curves for nanocrsytalline $Fe_2Mn_{1-x}Cu_xAl$ powders in the field H=100 Oe.

x=0.0, x=0.1 and x=0.3, respectively.

To further understand the magnetic properties an the type of the phase-transition in the nanocsrytalline $Fe_2Mn_{1-x}Cu_xAl$ powders, we have studied their isothermal magnetization curves at various temperatures around T_C, $M(H, T)$, see Fig. 3(a)–(c). One can see that the magnetization in the FM region does not reach saturation even at magnetic field up to 10 kOe. This feature can be due to the presence of magnetic disorder, magnetic inhomogeneity and/or anti-FM clusters in the samples. At a given H, the magnetization value decreases with increasing temperature. The FM nonlinear $M(H)$ curves become linear when the sample enters the PM region. This magnetic phase separation can be seen more clearly if H/M is plotted versus M^2 (corresponding to inverse Arrott plots of M^2 versus H/M) [21]. The nonlinear parts in the low-field region at temperatures below and above T_C are driven towards two opposite directions, see Fig. 3(d)–(f), revealing the FM–PM separation. According to Banerjee's criteria [22], if some H/M versus M^2 curves of a material show a negative slope, it exhibits the first-order phase transition (FOPT), while a positive slope corresponds to the second-order phase transition (SOPT). Comparing with these conditions reveals the FM–PM transitions of nanocsrytalline $Fe_2Mn_{1-x}Cu_xAl$ powders belonging to the SOPT, see Fig. 3(d)–(f).

According to the mean-field theory (MFT) proposed for a FM undergoing the SOPT and long-range FM interactions, the Landau free energy G_L is expanded in even powers of M [23]

$$G_L = aM^2 + bM^4 + \ldots\ldots - HM \quad (1)$$

where a and b are temperature dependent parameters. By minimizing G_L (dG_L/dM=0), we can obtain the relation

$$H/M = 2a + 4bM^2 \quad (2)$$

Eq. (2) implies that if magnetic interactions in a FM system exactly obey the MFT, the M^2 versus H/M curves in the vicinity of T_C are straight lines. However, this feature is only observed in Fig. 3(f), whereas it is not observed in Figs. 3(d) and 3(e). This result suggests an existence of short-range FM order in x=0.0 and 0.1 samples, while a long-range FM order exists in x=0.3 sample.

To determined the critical exponents (β, γ, and δ) and T_C for nanocsrytalline $Fe_2Mn_{1-x}Cu_xAl$ samples, we tried to analyze the $M(H)$ data according to the MAP method based on the Arrot–Noakes equation of state $(H/M)^{1/\gamma}=a\varepsilon+bM^{1/\beta}$, where $\varepsilon=(T-T_C)/T_C$ is the reduce temperature [17]. This equation implies that with correct β and γ values the performance of $M^{1/\beta}$ versus $(H/M)^{1/\gamma}$ curves in the vicinity of T_C introduces parallel straight lines, and one of those lines passes through the coordinate origin at T_C. It is known that the SOPT near T_C is characterized by the critical exponents of β (associated with the spontaneous magnetization, M_S), γ (associated with the initial magnetic susceptibility, χ_0^{-1}), and δ

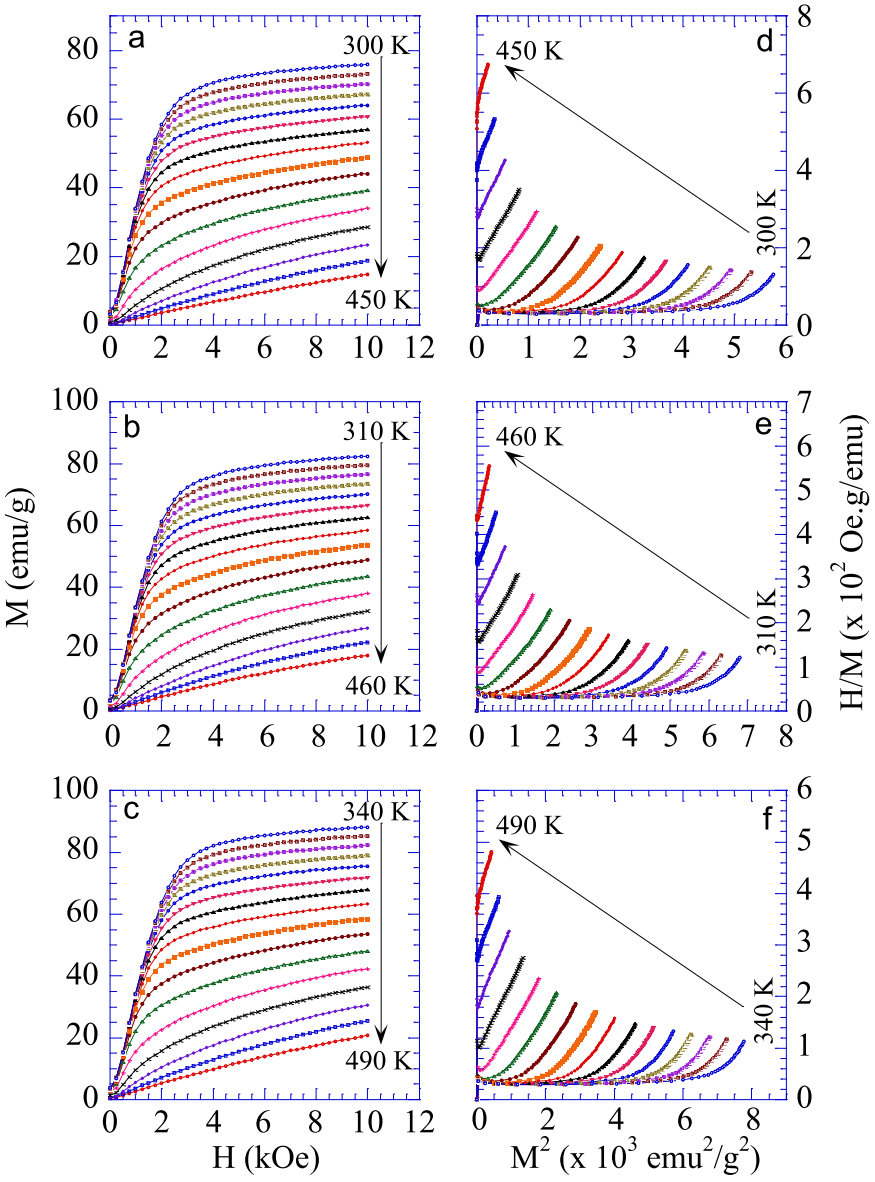

Fig. 3. (a)–(c) $M(H)$ curves and (d)–(f) H/M versus M^2 curves of nanocrsytalline $Fe_2Mn_{1-x}Cu_xAl$ powders, where $x=0.0$ (a) and (d), $x=0.1$ (b) and (e), $x=0.3$ (c) and (f).

(associated with the critical isotherm). These parameters obey the following relations [21]:

$$M_S(T) = M_0(-\varepsilon)^{\beta}, \quad \varepsilon < 0 \tag{3}$$

$$\chi_0^{-1}(T) = (h_0/M_0)\varepsilon^{\gamma}, \quad \varepsilon > 0 \tag{4}$$

$$M = DH^{1/\delta}, \quad T = T_C \tag{5}$$

where M_0, h_0/M_0, and D are the critical amplitudes. According to the MAP [17], values of $M_S(T)$ and $\chi_0^{-1}(T)$ are determined by plotting $M^{1/\beta}$ versus $(H/M)^{1/\gamma}$. In our case, maybe the values of β and γ describing the nanocsrytalline $Fe_2Mn_{1-x}Cu_xAl$ samples will be different from those expected for the MFT (with $\beta=0.5$ and $\gamma=1.0$ [21]) because of the existence of short-range FM order in the samples with $x=0.0$ and 0.1, as mentioned above. The content of the MAP in determining accurate values of β and γ can be briefly described as follows. Starting from initial trial values of $\beta=0.5$ and $\gamma=1.0$, the $M_S(T)$ and $\chi_0^{-1}(T)$ data obtained from the linear extrapolation are then fitted to Eqs. (3) and (4), respectively, to achieve better β, γ, and T_C values. These new values are continuously used for the next MAP to optimize their value. After iterating this process several times, β, γ, and T_C converge to stable values. $M_S(T)$ and $\chi_0^{-1}(T)$ data fitted to Eqs. (3) and (4), respectively, with critical exponents obtained from the final step of MAP are shown in Fig. 4(a)–(c). This procedure gives accurate values of β, γ, and T_C for samples as shown in Table 1. For the critical exponent of δ, it can be obtained by using the Widom scaling relation [21]

$$\delta = 1 + \gamma/\beta \tag{6}$$

From the values of β and γ for samples above obtained results, values of δ are calculated to be 3.6, 3.6, and 3.1 for $x=0.0$, 0.1, and 0.3, respectively.

The reliability of the obtained critical parameters can be verified by using the static-scaling theory, which predicts that the isothermal magnetization is a universal function of ε and H [21]:

$$M(H, \varepsilon) = \varepsilon^{\beta} f_{\pm}(H/\varepsilon^{\beta+\gamma}) \tag{7}$$

where f_+ for $T > T_C$ and f_- for $T < T_C$ are regular functions. Eq. (7) implies that the behavior of the $M/|\varepsilon|^{\beta}$ vs. $H/|\varepsilon|^{\beta+\gamma}$ curves is such

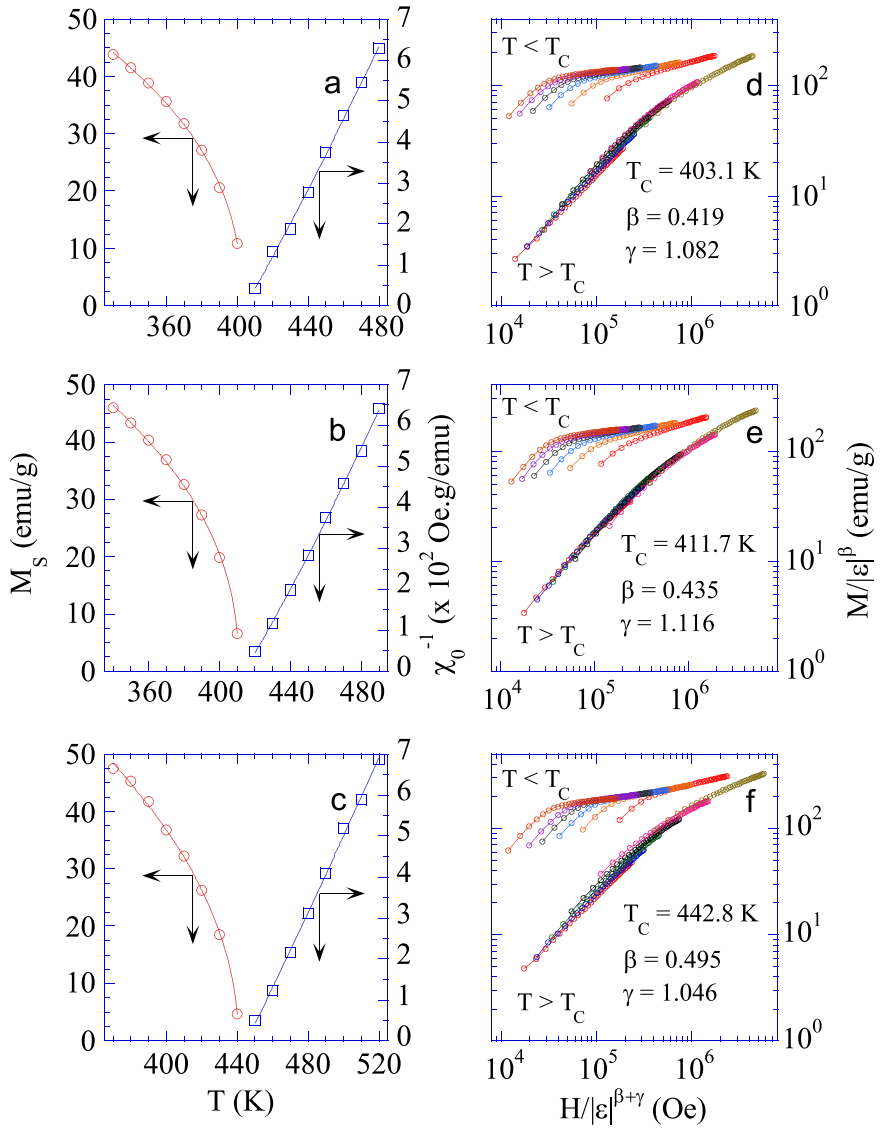

Fig. 4. (a)–(c) $M_S(T)$ and $\chi_0^{-1}(T)$ curves, (d)–(f) $M/|\varepsilon|^{\beta}$ versus $H/|\varepsilon|^{\beta+\gamma}$ plots in the log–log scale for nanocrsytalline $Fe_2Mn_{1-x}Cu_xAl$ powders, where $x=0.0$ (a) and (d), $x=0.1$ (b) and (e), $x=0.3$ (c) and (f).

Table 1
The values of the critical exponents of nanocrystalline $Fe_2Mn_{1-x}Cu_xAl$ powders compared with those of the theoretical models. Abbreviations: MAP: Modifined Arrott plots; K–F: Kouvel–Fisher method.

Models/material	Method	β	γ	δ	T_C[a] (K)	Ref.
Mean field theory		0.5	1.0	3.0	–	[21]
3D-Heisenberg model		0.365	1.336	4.7	–	[21]
3D-Ising model		0.325	1.241	4.8	–	[21]
Tricritical mean field theory		0.25	1.0	5.0	–	[24]
$x=0.0$	MAP	0.419 ± 0.012	1.082 ± 0.051	3.6 ± 0.1	403.1	This work
	K–F	0.414 ± 0.011	1.011 ± 0.041	3.4 ± 0.1	403.1	This work
$x=0.1$	MAP	0.435 ± 0.011	1.116 ± 0.042	3.6 ± 0.1	411.7	This work
	K–F	0.429 ± 0.013	1.101 ± 0.053	3.6 ± 0.1	411.0	This work
$x=0.3$	MAP	0.495 ± 0.015	1.046 ± 0.035	3.1 ± 0.1	442.8	This work
	K–F	0.487 ± 0.015	1.077 ± 0.046	3.2 ± 0.1	441.8	This work

[a] Values are obtained from critical behavior analyses.

that all $M(H, T)$ data points fall on two universal branches characteristic of f_+ for $T > T_C$ and f_- for $T < T_C$. For our case, by plotting the $M/|\varepsilon|^{\beta}$ versus $H/|\varepsilon|^{\beta+\gamma}$ data on a log–log scale and using the critical exponents and the T_C obtained from the MAP method, we can see that all the data fall onto two universal branches with $T > T_C$ and $T < T_C$, see Fig. 4(d)–(f). This reflects that the critical parameters β, γ, and T_C determined as described above are reliable. Notably, there is a small deviation of the $M(H, T)$ data

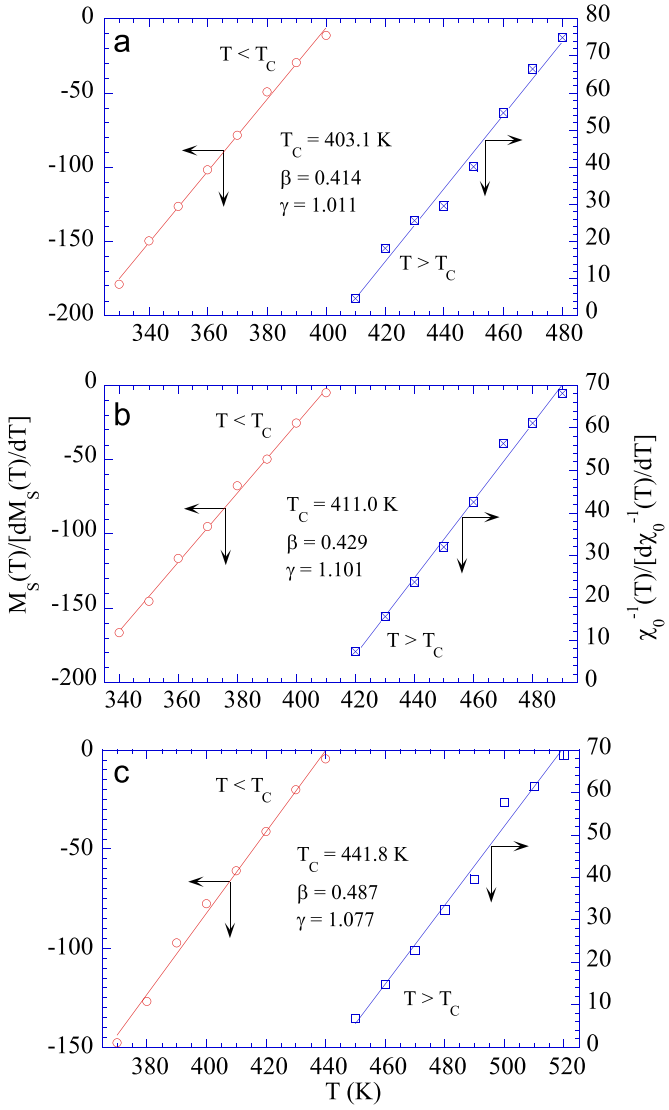

Fig. 5. Kouvel–Fisher plot of nanocrsytalline $Fe_2Mn_{1-x}Cu_xAl$ powders for (a) $x=0.0$, (b) $x=0.1$ and (c) $x=0.3$.

from the universal curves in the $M/|\varepsilon|^{\beta}$ versus $H/|\varepsilon|^{\beta+\gamma}$ performance at low fields ($H<4$ kOe), which is related to the rearrangement of magnetic domains where magnetic moments are not completely aligned to the field.

Alternatively, the values of β, γ, and T_C can be determined by the K–F method [18]. Using this method, the critical exponents β and γ could be independently determined. The K–F linear relations thus can be easily derived from Eqs. (3) and (4) as follows:

$$M_S(T)\left[dM_S(T)/dT\right]^{-1} = (T - T_C)/\beta \tag{8}$$

$$\chi_0^{-1}(T)\left[d\chi_0^{-1}(T)/dT\right]^{-1} = (T - T_C)/\gamma \tag{9}$$

The K–F method consists of an iterative procedure, which starts by constructing the Arrott–Noakes plot (i.e., the plot of $M^{2.5}$ versus $(H/M)^{0.75}$ [17]). According to the K–F method, plots of $M_S(dM_S/dT)^{-1}$ versus T and $\chi_0^{-1}(d\chi^{-1}/dT)^{-1}$ versus T should yield straight lines with slopes $1/\beta$ and $1/\gamma$, respectively. By the extrapolation, these straight lines give intercepts on the T axis equal to the T_C. Detailed descriptions of the K–F method can be found elsewhere [18]. The K–F plots of the final results for nanocsrytalline $Fe_2Mn_{1-x}Cu_xAl$ samples are shown in Fig. 5(a)–(c). The values of β, γ, and T_C for samples obtained from final step of K–F method are shown in Table 1. Using these β and γ values, the values of δ are found to be 3.4, 3.6, and 3.2 for $x=0.0$, 0.1, and 0.3, respectively, calculated from the Widom scaling relation, Eq. (6) [21]. One can see that the critical parameters obtained from bath the MAP and the K–F methods match well. This reflects that the values of β, γ, and T_C determined as described above are reliable.

Comparing the values of the critical exponents obtained for nanocsrytalline $Fe_2Mn_{1-x}Cu_xAl$ samples and of the theoretical models [21,24] is shown in Table 1. Clearly, the values $\beta=0.419$ and 0.435, $\gamma=1.082$ and 1.116 obtained by the MAP method and $\beta=0.414$ and 0.429, $\gamma=1.011$ and 1.101 obtained by the K–F method for $x=0.0$ and 0.1, respectively, are located between those of the MFT and the 3D-Heisenberg model. Whereas, the values $\beta=0.495$ and $\gamma=1.046$ obtained by the MAP method and $\beta=0.487$ and $\gamma=1.077$ obtained by K–F method for $x=0.3$ are more close to those expected for the MFT. However, the β values obtained are lower than $\beta=0.5$. These results suggest a coexistence of the short- and long-range FM interactions in these samples. Among these, long-range FM interaction could be associated with the core of nanocrystals. In contrast, short-range FM interaction corresponding to magnetic inhomogeneities in the samples are thought to surface-related effects, lattice strain and distortions, which lead to the weakening of the FM interaction strength. Notably, the β values obtained for Cu-doped samples shift towards that expected for the MFT. It means that Cu-doping into nanocsrytalline $Fe_2Mn_{1-x}Cu_xAl$ tends to result in long-range FM order. In other words, the samples become more magnetically homogeneous with increasing Cu-doping.

To get more information on critical properties of nanocsrytalline $Fe_2Mn_{1-x}Cu_xAl$ powders, we have also investigated the MCE of the samples via magnetic entropy change (ΔS_m) based on $M(H, T)$ data in vicinity of T_C shown in Figs. 3(a)–(c). It is known that the MCE is an intrinsic property and response of magnetic materials with respect to the application or removal of magnetic field, which is maximized near T_C. According to the thermodynamic theory, ΔS_m produced by the variation of a magnetic field variation from 0 to H is expressed by [21]

$$\Delta S_m(T,\ H) = \int_0^H \left(\frac{\partial M}{\partial T}\right)_H dH \tag{10}$$

Fig. 6(a)–(c) show $-\Delta S_m(T)$ curves of the samples under applied magnetic field changes $H=4$–10 kOe (with step of 2 kOe). For each sample at a given temperature, $|\Delta S_m|$ increase with increasing H. As a function of temperature, $-\Delta S_m(T)$ curve reaches a maximum value around T_C. With $H=10$ kOe, $|\Delta S_{max}|$ values of the samples are 0.58, 0.61, and 0.65 J kg^{-1} K^{-1} for $x=0.0$, 0.1, and 0.3, respectively.

Recently, a new method to describe T and H dependences of ΔS_m, $\Delta S_m(T, H)$, for SOPT materials has been introduced Franco and Conde [19]. According to this method, all $\Delta S_m(T)$ curves measured at different H values will collapse into a universal curve when $\Delta S_m(T)$ curves are normalized to their respective peak value (i.e., $\Delta S_m(T)/\Delta S_{max}$), and the temperature axis above and below T_C is rescaled as

$$\theta = (T - T_C)/(T_r - T_C) \tag{11}$$

where T_r is the reference temperature corresponding to a certain fraction k that fulfils $\Delta S_m(T_r)/\Delta S_{max}=k$. The choice of k does not affect the actual construction of the universal curve. In this work, we identified T_C as the temperature at the peak of the $-\Delta S_m(T)$ curve, and selected $k=0.6$ when constructing the universal curve for each sample. It means that T_r values are selected at $\Delta S_m(T_r)/\Delta S_{max}=0.6$ to rescale the temperature axis. Fig. 6(d)–

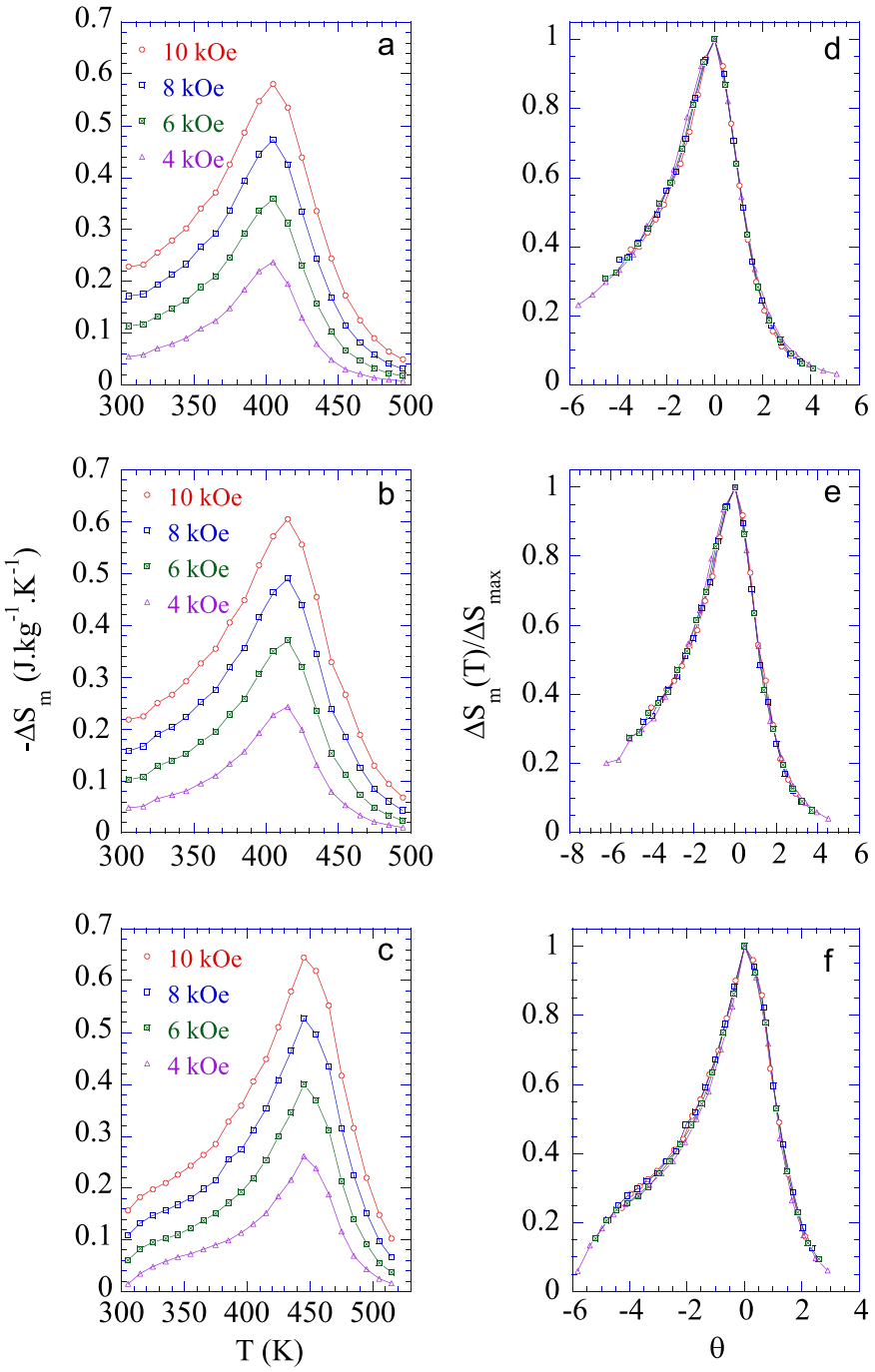

Fig. 6. (a)–(c) $-\Delta S_m(T)$ curves at different fields ranging from 4 to 10 kOe with step 2 kOe, (d)–(f) universal master curves for nanocrsytalline $Fe_2Mn_{1-x}Cu_xAl$ powders, where $x=0.0$ (a) and (d), $x=0.1$ (b) and (e), $x=0.3$ (c) and (f).

(f) shows the universal master curves for nanocsrytalline $Fe_2Mn_{1-x}Cu_xAl$ powders measured at different $H=4$–10 kOe. Clearly, the overlap of the different curves is reasonable in the whole temperature range. It means that the $\Delta S_m(T, H)$ data for nanocsrytalline $Fe_2Mn_{1-x}Cu_xAl$ powders follow a universal curve for magnetic entropy change. This is a familiar character of the SOPT material [25]. The overlap of $\Delta S_m(T, H)$ data into a unique curve is an additional confirmation of the general validity of the treatment in SOPT materials.

4. Conclusion

Critical properties of nanocsrytalline $Fe_2Mn_{1-x}Cu_xAl$ powders with $x=0$, 0.1, and 0.3 prepared by the high energy ball milling technique were investigated in detailed. Our experimental results demonstrated the FM–PM phase transition in the samples to be SOPT with critical exponents $\beta=0.419$–0.495, $\gamma=1.046$–1.116 obtained by MAP method and $\beta=0.414$–0.487, $\gamma=1.011$–1.101 obtained by K–F method. These values are not belonging to any universality class. They are located between those of the MFT and the 3D-Heisenberg model suggesting a coexistence of short- and long-range FM order in the samples. The samples become more magnetically homogeneous with increasing Cu-doping. Additionally, the $\Delta S_m(T)$ data measured at different applied magnetic field changes are collapsed into a universal master curve by normalizing $\Delta S_m(T)/\Delta S_{max}$ versus $\theta=(T-T_C)/(T_r-T_C)$. The follow a

universal curve of $\Delta S_m(T, H)$ data is an additional confirmation the the FM–PM transitions of nanocsrytalline $Fe_2Mn_{1-x}Cu_xAl$ powders belonging to the SOPT.

Acknowledgments

This research was supported by the Converging Research Center Program through the Ministry of Science, ICT and Future Planning, Korea (2014048835).

References

[1] S. Chen, Z. Ren, Mater. Today 16 (2013) 387.
[2] K. Bartholomé, B. Balke, D. Zuckermann, M. Köhne, M. Müller, K. Tarantik, J. König, J. Electron. Mater. 43 (2014) 1775.
[3] F. Casper, T. Graf, S. Chadov, B. Balke, C. Felser, Semicond. Sci. Technol. 27 (2012) 063001.
[4] C. Wang, J. Meyer, N. Teichert, A. Auge, E. Rausch, B. Balke, A. Hütten, G. H. Fecher, C. Felser, J. Vac. Sci. Technol. B 32 (2014) 020802.
[5] Y. Liu, X. Zhang, D. Xing, H. Shen, D. Chen, J. Liu, J. Sun, J. Alloy. Compd. 616 (2014) 184.
[6] Y.V.B. de Santanna, M.A.C. de Melo, I.A. Santos, A.A. Coelho, S. Gama, L.F. Cótica, Sol. State Commun. 148 (2008) 289.
[7] V. Basso, C.P. Sasso, K.P. Skokov, O. Gutfleisch, V.V. Khovaylo, Phys. Rev. B 85 (2012) 014430.
[8] M.I. Katsnelson, V.Y. Irkhin, L. Chioncel, A.I. Lichtenstein, R.A. de Groot, Rev. Mod. Phys. 80 (2008) 315.
[9] I. Žutić, J. Fabian, S. Das Sarma, Rev. Mod. Phys. 76 (2004) 323.
[10] Y. Sakuraba, M. Hattori, M. Oogane, Y. Ando, H. Kato, A. Sakuma, T. Miyazaki, H. Kubota, Appl. Phys. Lett. 88 (2006) 192508.
[11] I. Galanakis, P. Mavropoulos, P.H. Dederichs, J. Phys. D: Appl. Phys. 39 (2006) 765.
[12] I. Galanakis, P. Mavropoulos, J. Phys.: Condens. Matter 19 (2007) 315213.
[13] C. Felser, G.H. Fecher, B. Balke, Angew. Chem. Int. Ed. 46 (2007) 668.
[14] W.J. Feng, Q. Zhang, L.Q. Zhang, B. Li, J. Du, Y.F. Deng, Z.D. Zhang, Solid State Commun. 150 (2010) 949.
[15] N.H. Duc, T.D. Thanh, N.H. Yen, P.T. Thanh, N.H. Dan, T.L. Phan, J. Korean Phys. Soc. 60 (2012) 454.
[16] W. Zhu, E.K. Liu, L. Feng, X.D. Tang, J.L. Chen, G.H. Wu, H.Y. Liu, F.B. Meng, H. Z. Luo, Appl. Phys. Lett. 95 (2009) 222512.
[17] A. Arrott, J.E. Noakes, Phys. Rev. Lett. 19 (1967) 786.
[18] J.S. Kouvel, M.E. Fisher, Phys. Rev. 136 (1964) A1626.
[19] V. Franco, A. Conde, Int. J. Refrig. 33 (2010) 465.
[20] T. Graf, C. Felser, S.S.P. Parkin, Prog. Solid State Chem. 39 (2011) 1.
[21] H.E. Stanley, Introduction to Phase Transitions and Critical Phenomena, London Oxford University Press, London, 1971.
[22] S.K. Banerjee, Phys. Lett. 12 (1964) 16.
[23] J.M.D. Coey, Magnetism and Magnetic Materials, Cambridge University Press, NewYork, 2010.
[24] D. Kim, B. Revaz, B.L. Zink, F. Hellman, J.J. Rhyne, J.F. Mitchell, Phys. Rev. Lett. 89 (2002) 227202.
[25] C.M. Bonilla, J.H. Albillos, F. Bartolome, L.M. Garcia, M.P. Borderias, V. Franco, Phys. Rev. B 81 (2010) 224424.